SEISMIC BEHAVIOUR OF REINFORCED CONCRETE WALLS WITH MINIMUM VERTICAL REINFORCEMENT

Yiqiu Lu and Richard Henry

The University of Auckland, Auckland, 1142, New Zealand

Abstract

Recent research suggested that the current minimum vertical reinforcement limits in NZS 3101:2006 may be insufficient to ensure well distributed cracks in plastic hinge regions. A series of numerical analyses were used to investigate the behaviour of an example RC wall designed according to the minimum requirements in several different concrete design standards. The analysis results confirmed the observed failure mode of an RC wall damaged during the Canterbury earthquakes that had only half the current required minimum vertical reinforcement. Furthermore, RC walls built in accordance with current minimum vertical reinforcement requirements in both ACI 318-11 and NZS 3101: 2006 were shown to still be susceptible to limited flexural cracking and premature bar fracture. In addition to the modelling, six large-scale walls have been tested to examine the effect of axial load, shear span ratio, and reinforcement ties in the end region on RC walls with distributed minimum vertical reinforcement in accordance with NZS 3101:2006. The observed extent of crack distribution, hysteretic behaviour, failure mode, and drift capacity of four of the tested walls are discussed. The experimental results confirmed that current minimum vertical reinforcing limits in NZS 3101:2006 are insufficient to form a large number of secondary cracks. The failure mode for all walls was controlled by bar buckling and subsequent fracture. The lateral drift capacity of all four tested walls was 2.5% and both the shear span ratio and the anti-buckling ties had no significant influence on the drift capacity.

Keywords: Bar Buckling, Cracks, Experimental testing, Finite Element Modelling, Minimum Vertical Reinforcement, Reinforced Concrete Wall

1 Introduction

Severe damage was observed to reinforced concrete (RC) walls in some modern multi-storey buildings during the 2010/2011 Canterbury earthquake in New Zealand. In particular, several lightly reinforced concrete walls in multi-storey buildings formed a limited number of cracks in the plastic hinge region as opposed to the expected distributed cracking (Kam, Pampanin & Elwood 2011; Structural Engineering Society of New Zealand (SESOC) 2011; Sritharan & al. 2014). This behaviour is typical of RC walls with low vertical reinforcement contents. If insufficient vertical reinforcement is provided in RC walls, the tension force generated by the reinforcing steel may be insufficient to develop secondary flexural cracks in the surrounding concrete (Henry 2013). This behaviour can lead to a limited number of cracks in the plastic hinge region at the wall base. The inelastic deformation will concentrate over a short plastic hinge length, resulting in premature fracture of vertical reinforcement. Examples of RC walls with distributed crack and RC walls with limited cracks following the Canterbury Earthquakes are shown in Fig. 1. In response to the observed performance of lightly reinforced RC walls, the Canterbury Earthquakes Royal Commission (CERC) highlighted the need for further research to ensure yielding of reinforcement can extend over a significant height of the wall rather than just the immediate vicinity of a limited number of primary cracks.




(a) Well distributed flexural cracks (Kam et al. 2011) | (c) Few flexural cracks (Credit: Charles Clifton) | (c) Few flexural cracks (Credit: Ken Elwood) | (d) Fractured bars (Credit: Des Bull)

Fig. 1 Examples of observed damage to well detailed and lightly reinforced concrete walls

Minimum reinforcement requirements for RC walls are imposed by most concrete design standards worldwide. Requirements for vertical reinforcement ratio not only imposed to mitigate shrinkage and temperature effects, but also intended to prevent non-ductile failure modes such as a flexural single crack formation. Recent research suggests that the current minimum vertical reinforcement limits in New Zealand concrete structures standard, NZS 3101 (2006) may be insufficient to ensure well distributed cracking in ductile plastic hinge regions, resulting in premature bar fracture, and low drift capacities (Henry 2013).

Although a significant amount of research has been carried out into the seismic behaviour of RC walls, there have been limited experimental testing or modelling of flexure dominant RC walls with low reinforcement ratios representative of many RC walls worldwide. A series of numerical analyses were conducted to investigate the behaviour of one of the RC walls in the Gallery Apartment building that was damaged during the Canterbury earthquakes and walls designed according to minimum requirements from different concrete design standards. In addition, a total of six large scaled walls were tested to examine the effect of axial load, shear span ratio, and transverse reinforcement in the end region on the seismic performance of RC walls with distributed minimum vertical reinforcement in accordance with NZS 3101:2006. The modelling analysis results and the preliminary results from four test walls are presented.

2 Numerical modelling

2.1 Model description

A series of numerical analyses were conducted to investigate the lateral load response of RC walls with minimum reinforcement using nonlinear finite element program VecTor2 (Wong & Vecchio 2003). Several researches have previously validated the accuracy of VecTor2 for modelling the lateral load behaviour of RC walls (Ghorbani-Renani & al. 2009; Luu & al. 2013). In this study, four–node plane stress rectangular elements were used to model the RC walls with smeared horizontal and vertical reinforcement. Axial compression due to gravity loads was held constant during the analyses, whereas the lateral load applied at the top of the wall was monotonically increased in a displacement-control mode until failure. The constitutive law for concrete in compression uses the Hognestad parabola model with a Park-Kent (Park, Priestley & Gill 1982) descending branch. The fib Model Code recommendation was adopted for the uniaxial tensile strength of the concrete (Fédération Internationale du Béton (fib) 2012) and a tri-linear stress-strain response was used for the reinforcement. Detailed descriptions of the material models can be found in the VecTor2 user manual (Wong & Vecchio 2003).

The grid-F wall from the Gallery Apartments building in Christchurch was used as the baseline for the VecTor2 analyses. The grid-F wall had a length of 4300 mm, a thickness of 325 mm, two

layers of DH12 vertical reinforcement at 460 mm centers and DH12 horizontal reinforcement at 400 mm centers. The vertical reinforcement ratio for the as-built grid-F wall was 0.16%, less than the 0.27% currently required by NZS 3101:2006 as the minimum vertical reinforcement was only required to exceed 0.14% when Gallery Apartment building was designed. The grid-F wall was 39 m high corresponding to shear span ratio of 6.1 when using an inverse triangular lateral force distribution. Tests performed on two concrete cores extracted from the building indicated compressive strengths of 46.5 and 56.0 MPa. As a result, the as-built grid-F model was analysed using the average measured concrete strength of 51.3 MPa with a corresponding tensile strength of 4.34 MPa. The reinforcement properties had a yield strength of 560 MPa, an ultimate strength of 690 MPa and an ultimate strain of 12.9%. The axial load acting on the grid-F wall was 2250 kN, corresponding to an axial load ratio of 3.0%.

Additional analyses were conducted using the dimensions of the grid-F wall with modified reinforcement detailing in accordance with the current minimum requirements from different concrete standards worldwide, including New Zealand concrete structures standard NZS 3101:2006 (NZS) (2006), the US building code requirements for structural concrete ACI 318-11 (ACI) (2011), the European seismic design standard Eurocode 8 (Eurocode) (CEN 2004), the Canadian concrete structural design standard CSA A23.3 standard (CAS) (2004), and the Chinese concrete design standard GB 50010 (GB) (2010). The lengths of the boundary element or end region of Eurocode, CAS and GB were taken as $0.15l_w$, which was equal to 645 mm. The concrete strength was defined as the specified 28-day concrete strength of 30 MPa, with a corresponding tensile strength of 2.93 MPa. The reinforcing steel properties were kept the same as that described for the as-built grid-F wall. The minimum requirement and the resulting reinforcement contents for each of the walls modelled are summarised in Table 1. The walls designed in accordance with ACI and NZS had evenly distributed vertical reinforcement, whereas the walls designed in accordance with Eurocode, CAS and GB had additional reinforcement lumped in end regions (boundary elements) with distributed reinforcement along the web region.

Table 1
Summary of reinforcement requirements and details of each of the walls modelled

Standards	Requirement		reinforcement ratio		
	Total/distributed reinforcement ratio	End region reinforcement ratio	End region reinforcement ratio ρ_b	Web reinforcement ratio ρ_w	Total reinforcement ratio
As-built grid-F	$0.7/f_y$	No requirement	-	0.16%	0.16%
ACI 308-11	>0.25%	No requirement	-	0.254%	0.254%
NZS 3101: 2006	$>\sqrt{f_c'}/4f_y$	No requirement	-	0.275%	0.275%
Eurocode 8	>0.2%	>0.5%	0.5%	0.2%	0.29%
CSA 2004	>0.25%	$>(0.15\%b_w l_w)/(b_w l_b)$	1.0%	0.254%	0.48%
GB 50010-2010	>0.25%	>1.0%	1.0%	0.254%	0.48%

2.2 Modelling results

Fig. 2 and Fig. 3 show the predicted crack patterns and lateral force-drift response calculated for each of the walls modelled. The behaviour of the modelled as-built grid-F wall was similar to the

failure mode observed during the 22 Feb 2011 Christchurch earthquake, with a single flexural crack at the wall base. The strain in the vertical reinforcement was concentrated at the single crack and not distributed along a large length of the bar. Because of the reduced spread of the plasticity, the wall demonstrated only limited ductility with fracture of vertical reinforcement occurring at only 0.75% lateral drift.

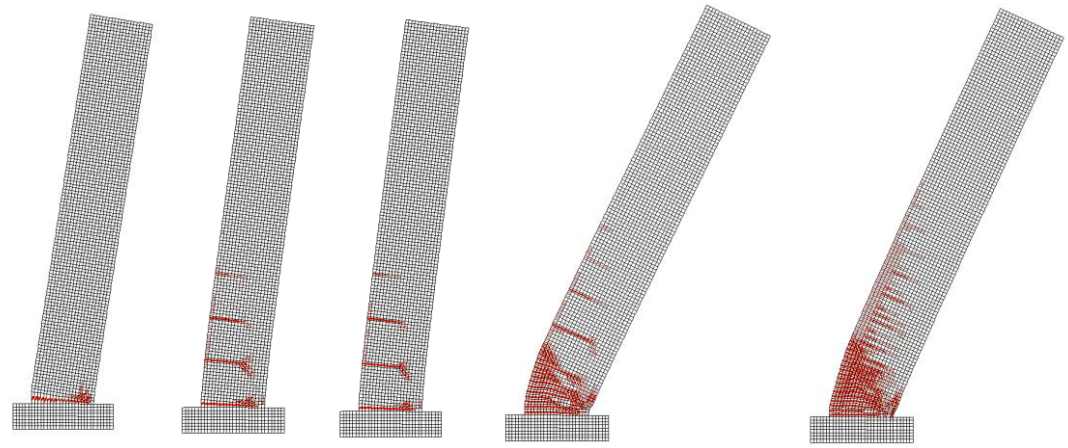

(a) Grid-F (b) ACI (c) NZS (d) Eurocode (e) CAS & GB

Fig. 2. Deformed shape (magnified x5) and crack patterns of each of the walls modelled

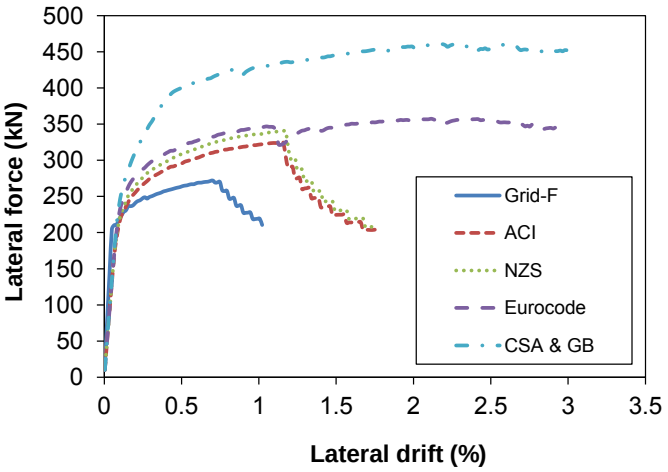

Fig. 3. Calculated lateral force-drift response for each of the walls modelled

All of the walls designed in accordance with current design standards showed an improved lateral-load response when compared to the as-built grid-F wall. The crack patterns for the walls designed according to both ACI and NZS were similar with a total of four primary flexural cracks developing. The reinforcement ratio of these two walls was 58% and 72% higher than the as-built grid-F wall. However, despite the increased number of flexural cracks in the ACI and NZS walls, the reinforcement was still insufficient to generate a large number of secondary cracks and fracture of the vertical reinforcement occurred at a modest 1.2% lateral drift. The calculated displacement capacity for the ACI and NZS walls was significantly less than the allowable drift limits for ductile buildings.

The performance of the wall designed in accordance to Eurocode was significantly better than the walls designed according to ACI and NZS. The concentrated reinforcement ratio of 0.5% in the end regions of the wall was sufficient to generate a large number of secondary cracks in the plastic hinge region, as shown in Fig. 2-d. However, because the total reinforcement for the Eurocode wall is not significantly larger than the NZS wall, the maximum lateral strength was similar, as shown in

Fig. 3. The increased secondary cracking in the Eurocode wall improved the spread of inelastic strains in the vertical reinforcement, resulting in a significantly more ductile response than that calculated for the ACI or NZS walls. The Eurocode wall indicates that concentrating a greater portion of reinforcement at the wall ends could result in a significant improvement in the seismic response of lightly reinforced concrete walls.

The performance of walls designed with CSA and GB are similar with Eurocode. Because the distributed and boundary reinforcement are both larger than Eurocode, the maximum lateral strength is higher than Eurocode. In addition, secondary cracks are denser both in the boundary elements and web region in the plastic hinge region and also distribute along a greater height of the wall.

3 EXPERIMENTAL INVESTIGATION

The model analysis show that the vertical reinforcement in the wall designed in accordance with ACI and NZS 3101: 2006 was insufficient to generate a large number of distributed cracks, resulting in premature bar fracture, and low drift capacities. To validate the numerical modelling a series of experimental tests were conducted. The first phase test focused on evaluating the current minimum vertical reinforcement limits in NZS 3101:2006. Six large-scale RC cantilever test walls that were subjected to pseudo-static cyclic loading were tested in University of Auckland. A summary of the six test walls is shown in Table 2, and drawings of the cross sections of the wall specimens are shown in Fig. 4. The 1.4 m long, 2.8 m high and 150 mm thick wall specimen were designed to approximately represent a 40-50% scale version of RC walls with limited ductility as per NZS 3101:2006. The vertical reinforcement was identical for all six walls and designed in accordance with minimum requirement in NZS 3101:2006, which is $\rho_n \geq \sqrt{f_c'}\big/\left(4 f_y\right)$. Three shear span ratios will be applied to the test walls, 2, 4, and 6, representing walls in a range of different building heights. The applied axial load was also varied from 0-7% of the wall axial capacity. The axial load for wall C5 triggered the NZS 3101:2006 requirement for additional confinement reinforcement in the end regions to achieve a limited ductile response. Wall C6 was identical with Wall 2 expect that stirrups to provide anti-buckling restraint were added in the wall end region.

Because of height limitations in the structural test hall, a test setup was designed to simulate the expected seismic loading on the bottom two storeys of a 40-50% scaled wall from a multi-storey building. Based on an assumed lateral-load distribution, the moment, shear, and axial loads at the second storey height can be calculated, as shown in Fig. 5. The test setup developed for the RC wall specimen is shown in Fig. 6. An actuator was attached between the steel loading beam and the strong wall to apply horizontal loads to the wall, and two additional actuators were attached vertically at each end of the wall to achieve the required moment and axial load at the top of the wall.

Table 2

Details of the RC test walls

Wall	Shear span ratio	Axial load ratio	Specified material properties		Vertical reinforcement ratio (%)	End stirrups (mm)
			f_c' (MPa)	f_y (MPa)		
C1	2	3.5%	40	300	0.53	No
C2	4	3.5%	40	300	0.53	No
C3	6	3.5%	40	300	0.53	No
C4	2	0	40	300	0.53	No
C5	2	7%	40	300	0.53	D6@90
C6	4	3.5%	40	300	0.53	D6@60

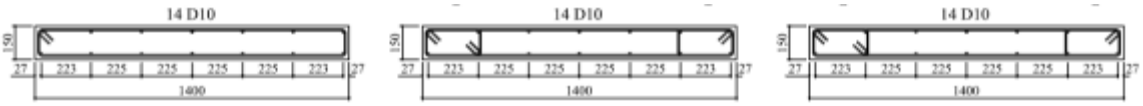

Fig. 4. Cross sections of test wall specimens

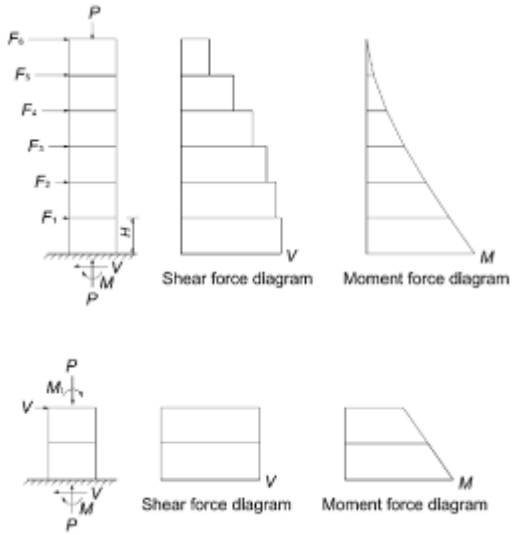

Fig. 5. Seismic loading on multi-storey RC walls

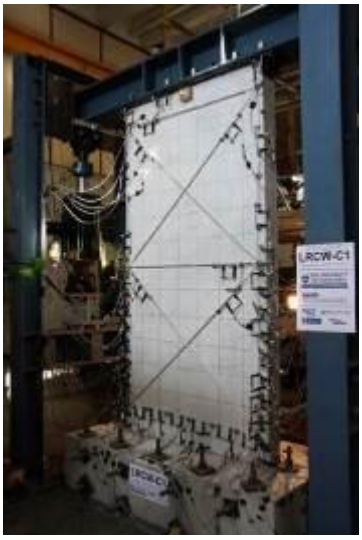

Fig. 6. Experimental test setup for RC walls

The loading protocol was in accordance with recent ACI standards (ACI ITG-5.1-07 2008). Several small load steps were applied below the calculated cracking moment of the section, followed by displacement controlled loading to specified lateral drifts. The loading protocol is shown in Fig. 7.

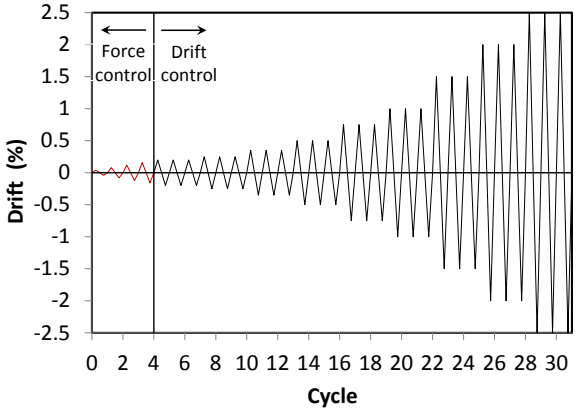

Fig. 7. Loading protocol applied to all test walls

4 Preliminary test results

The preliminary results of tests C1, C2, C3, and C6 are reported here. The overall condition of these four walls at the end of each test is shown in Fig. 8, the failure modes are shown in Fig. 9, and the measured moment-displacement hysteresis curves are plotted in Fig. 10. The tests were terminated after a 20% drop in the resistance at peak deformation compared to the maximum strength reached during the test (Park 1988). A brief description of the progression of the damage and the final failure mechanism is given for each test wall.

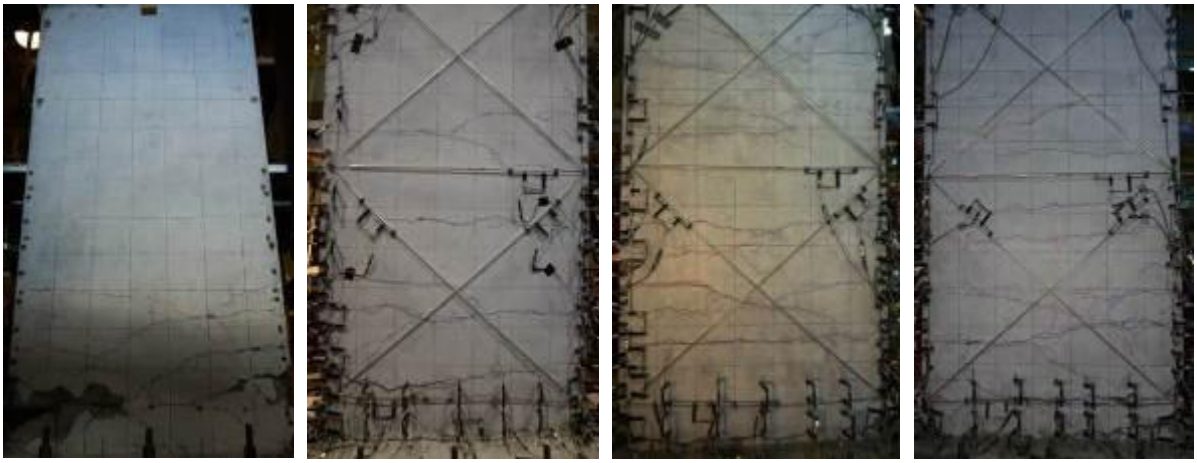

(a) Wall C1 (b) Wall C2 (c) Wall C3 (d) Wall C6

Fig. 8 Overall condition of four test walls after failure

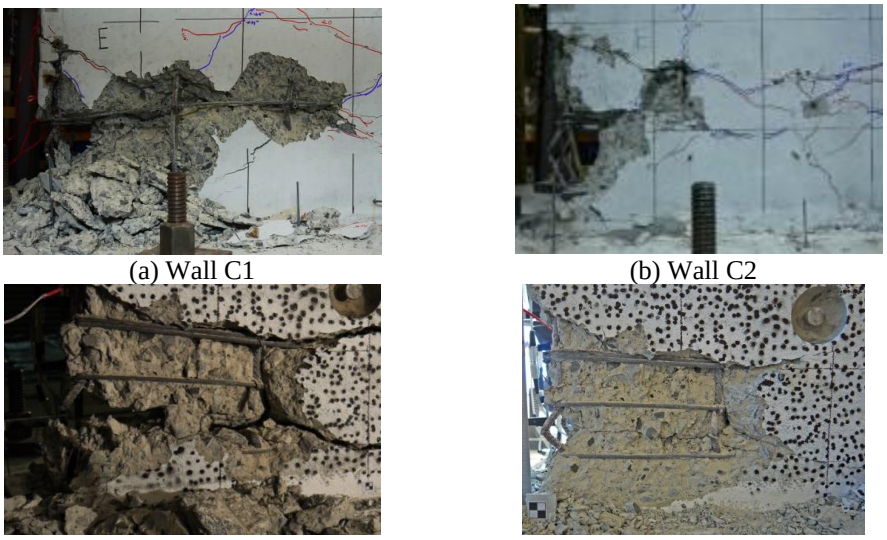

(a) Wall C1 (b) Wall C2

(c) Wall C3 (d) Wall C6

Fig. 9 Failure modes of the four test walls

4.1 Wall C1

The wall response was dominated by flexural behaviour with 3-4 main flexural cracks forming in the lower 1/4 the wall height, as shown in Fig. 8-a. These 3-4 cracks were triggered before the lateral drift of ±0.25%, after which no significant new flexural cracks occurred. During high lateral drift cycles, the wall deformation was primarily concentrated at a single crack which opened up to 20 mm wide with the other flexural cracks not opening wider than a few millimeters. The concrete at the corners of the wall started to spall at lateral drifts of ±1.0% and bar buckling initiated at the location of that large flexural crack during cycles to lateral drift of ±1.5%. Due to the lack of confinement reinforcement, the bar buckling accelerated concrete spalling and core crushing occurred during the first cycle to -2.5% drift, as shown in Fig. 9-a. Two corner bars fractured during the third cycle to +2.5% drift. Fig. 10-a shows the measured base moment-displacement response for wall C1. The uncracked wall had a high initial cross section stiffness and the first flexural crack did not initiate until a lateral force of approximately 100 kN was reached, corresponding to a moment at the wall base of 280 kN-m, or roughly 55% of the peak strength. The inelastic response was stable up until 1.5% lateral drift when bar buckling occurred causing strength degradation on subsequent cycle. A drop of 20% of the peak strength occurred when the core crushed during the first cycles to -2.5% lateral drift. The strength degradation continued and two of the vertical reinforcing bars fractured on the third cycle to +2.5% lateral drift. The test was terminated after three cycles to ±2.5% lateral drift. Numerical models predicted that the vertical reinforcement would fracture earlier than that observed during the test (Lu, Henry & Ma 2014),

however, the spalling of cover concrete and bar buckling resulted in the reinforcement being stretched over a longer length than that predicted in the model which delayed vertical bar fracture.

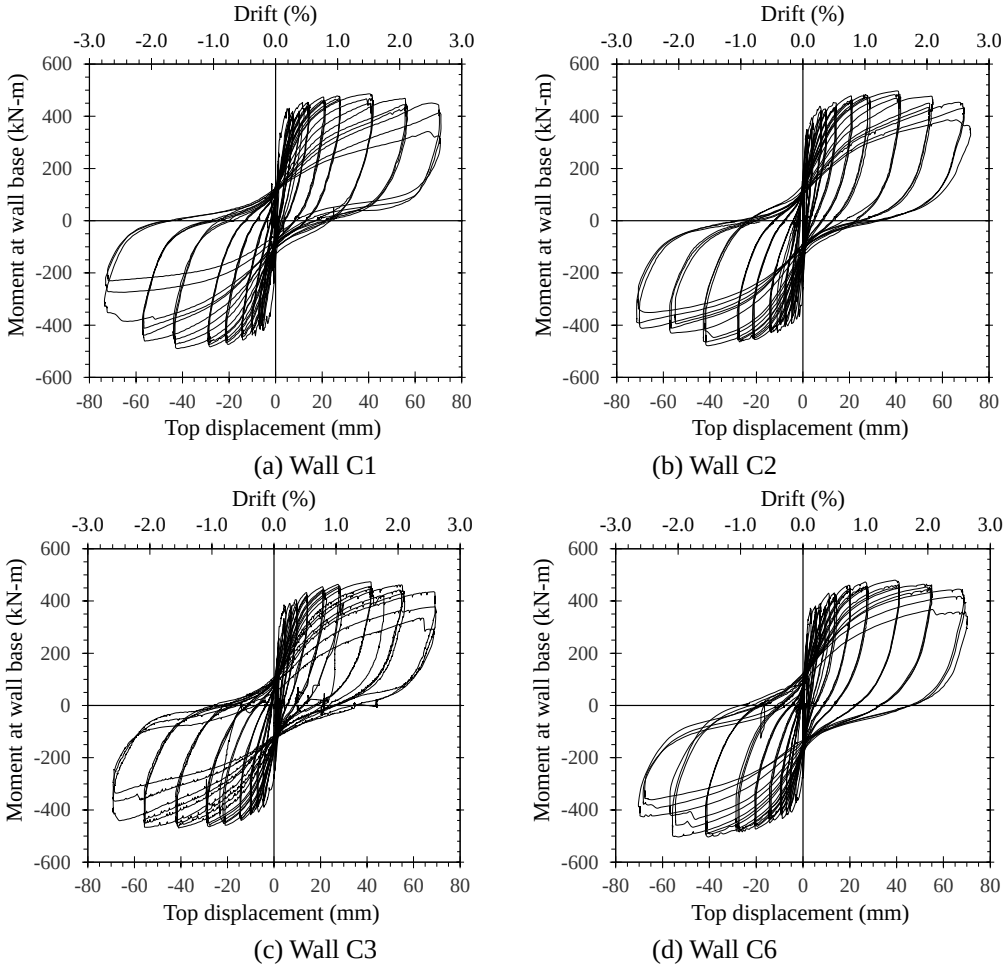

(a) Wall C1 (b) Wall C2

(c) Wall C3 (d) Wall C6

Fig. 10 Hysteric curves of six test walls

4.2 Wall C2

Test wall C2 was identical to wall C1 expect that the shear span ratio was increased from 2 to 4 meaning that a moment was applied to the top of the wall in addition to the lateral force. With the higher shear span ratio, the flexural cracks extended higher than wall C1, up to 3/4 of the wall height, as shown in Fig. 8-b. However, the wall response was still dominated by 3-4 large flexural cracks at the wall base, with most other cracks widths less than 2 mm in width. Similar to wall C1, all the flexural cracks formed prior to 0.5% lateral drift. The concrete in the east corner started to spall during the first cycle to -1.5% lateral drift, and buckling of vertical reinforcement initiated during the third cycle to ±1.5% lateral drift. The location of the bucking is the large crack place. During the cycles to ±2.0% lateral drift, bar buckling became more severely and crushing of the core concrete occurred. Two corner bars in east side fractured during the third cycle to +2.5% lateral drift and one bar fractured in west side during the third cycle to -2.5% lateral drift. The finial failure condition at east side of the wall is shown in Fig. 9-b. The measured moment-displacement response for wall C2 is shown in Fig. 10-b, with a similar response observed compared wall C1. The first flexural crack initiated during the first cycle to the drift of -0.06% at a lateral force of 62 kN corresponding to the wall base moment of 365 kN-m, or roughly 72% of the peak strength. The inelastic response was stable until ±1.5% when bar buckling occurred and caused a gradual degradation in wall strength. Two vertical bars fractured leading the strength dropped below 80% of the peak strength. When the wall was pulled back to -2.5%, the wall also experienced a large drop of strength in the other direction because of bar fracture.

4.3 Wall C3

Wall C3 was identical with walls C1 and C2 except that wall C3 has a shear span ratio of 6, representing a multi-story building wall. As shown in Fig. 8-c, the cracks extended over almost the whole wall height. Although a large number of cracks formed, the spacing of these cracks was large meaning these cracks were considered primary flexural cracks and no significant secondary cracking occurred between these primary cracks. Similar to wall C2, the behaviour of wall C3 was controlled by 3-4 main flexural cracks at the wall base. The lateral deformation was mostly attributed to these large flexural cracks. Concrete spalling and bar buckling were observed in the east corner during the first cycle to -1.5% lateral drift. During the cycles to ±2.0% lateral drift, bar buckling became more obviously and the core concrete started to crush in the east corner. During the second cycle to +2.5% lateral drift, one east corner bar fractured and one west corner bar was buckled to break off. During the third cycle to ±2.5% lateral drift, the other east and west corner bars fractured. The finial failure condition of wall C3 is shown in Fig. 9-c. The measured moment-displacement response for wall C3 is shown in Fig. 10-c, with a similar response observed compared with walls C1 and C2. A few flexural cracks initiated simultaneously during the first cycle to a drift of +0.16% at a lateral force of 43 kN corresponding to the wall base moment of 383 kN-m which is nearly 81% of the peak strength. Strength degradation also occurred after ±1.5% lateral drift because of bar buckling. During the second cycle to -2.5% lateral drift, the strength dropped below 80% of the peak strength due to one corner bar fracturing. From the test results of wall C1, C2 and C3, the increased shear span ratio did not appear to have a significant influence on the drift capacity of the wall.

4.4 Wall C6

Wall C6 was identical to wall C2 except that anti-buckling reinforcement was provided in the form of closely spaced stirrups in end region of wall. As shown in Fig. 8-d, the observed crack pattern for wall C6 was similar to that observed for wall C2. The flexural cracks extended over approximately 3/4 of the wall height, with 3-4 dominant cracks at the wall base. Despite the presence of the anti-buckling stirrups, the onset of concrete spalling and bar buckling was still observed at the west end of the wall during the third cycle to 1.5% lateral drift. The two buckled bars fractured during the second cycle and third cycle to the drift of 2.0%, causing a large drop of the strength. The east end spalled during the first cycle to -2.0% lateral drift but there was no sign of bar buckling until the third cycle to the drift of -2.0%. The buckled bar eventually fractured during the cycle to -2.5% lateral drift, leading to a 20% drop in wall strength. The finial failure mode on the east of the wall is shown in Fig. 9. The measured moment-displacement response for wall C6 is shown in Fig. 10-d. When the wall was pushed in the positive direction, the strength started to drop during cycles to 1.5% lateral drift, while in other direction the wall maintained a stable response until -2.0% lateral drift when bar buckling occurred. The lateral drift of 2.5% for wall C6 was the same as that observed for wall C1 and wall C2, indicating that the transverse reinforcement in the end region had little influence on the wall drift capacity.

5 Conclusions

An investigation was conducted to evaluate the minimum vertical reinforcement limits for RC walls. Monotonic analysis was conducted using nonlinear finite element program VecTor2 to investigate the behaviour of one of the RC walls in the Gallery Apartment building damaged during the Canterbury earthquakes, as well as walls designed according to minimum requirements from different concrete design standards. Moreover, a total of six large scaled walls were tested to examine the effect of axial load, shear span ratio, and end region stirrups on the seismic performance of RC walls with distributed minimum vertical reinforcement in accordance with NZS 3101:2006. Based on the analysis results of the modelled walls and the preliminary results from four tests, the following conclusions were drawn:

1. The behaviour of the modelled as-built grid-F RC wall in the Gallery Apartments Building confirmed the failure mode observed during the 22 Feb 2011 Christchurch earthquake, with a single flexural crack at the wall base and fracture of the vertical reinforcement.
2. The vertical reinforcement in the RC walls designed in accordance with ACI and NZS were insufficient to generate a large number of distributed cracks, resulting in premature bar fracture, and low drift capacities. The performance of the walls designed in accordance to

Eurocode, CSA and GB were significantly better than the walls designed according to ACI and NZS. Concentrated reinforcement in the end regions of RC walls may improve their ductility of lightly reinforcement walls.

3. The four test walls with current minimum vertical reinforcing requirements in NZS 3101:2006 were insufficient to form a large number of secondary cracks. The failure mode for all the test walls was controlled by bar buckling and subsequent fracture.
4. The lateral drift capacity of all four walls was 2.5%. Both the shear span ratio and the inclusion of anti-buckling ties in the wall end region had no significant influence on the drift capacity of the test walls.

Acknowledgement

Financial support for this research was provided by the Natural Hazards Research Platform through contract C05X0907 in addition to the Chinese Scholarship Council and the University of Auckland. The assistance of Ronald Gultom in helping the test is greatly appreciated.

Reference

ACI 318-11 (2011). Building Code Requirements for Structural Concrete (ACI 318-11) and Commentary. Farmington Hills, Michigan, American Concrete Institute.

ACI ITG-5.1-07 (2008). Acceptance Criteria for Special Unbonded Post-Tensioned Precast Structural Walls Based on Validation Testing and Commentary. Farmington Hills.

CEN (2004). Eurocode 8: Design of structures for earthquake resistance. Brussels, Belgium, European Committee for Standardization.

CSA (2004). Design of concrete structures. Standard CSA-A23.3-04. Toronto Canadian Standards Association.

Fédération Internationale du Béton (fib) (2012). Model Code 2010 - Final draft, Volume 1. fib Bulletin, 65. Lausanne, Switzerland.

GB 50010-2010 (2010). Code for design of concrete structures Beijing, China Architecture&Building Press.

Ghorbani-Renani, I., Velev, N., Tremblay, R., Palermo, D., Massicotte, B. and Léger, P. (2009). Modeling and testing influence of scaling effects on inelastic response of shear walls. ACI Structural Journal, Vol. **106**, No. 3: pp. 358-367.

Henry, R. S. (2013). Assessment of minimum vertical reinforcement limits for RC walls. Bulletin of the New Zealand Society for Earthquake Engineering, Vol. **46**, No. 2: pp. 88-96.

Kam, W. Y., Pampanin, S. and Elwood, K. J. (2011). Seismic performance of reinforced concrete buildings in the 22 Feburary Christchurch (Lyttelton) earthquake. Bulletin of the New Zealand Society for Earthquake Engineering, Vol. **44**, No. 4: pp. 239-278.

Lu, Y., Henry, R. S. and Ma, Q. T. (2014). Modelling and Experimental Plan of Reinforced Concrete Walls with Minimum Vertical Reinforcement Proceedings of the Tenth U.S. National Conference on Earthquake Engineering, Anchorage, Alaska.

Luu, H., Ghorbanirenani, I., Léger, P. and Tremblay, R. (2013). Numerical modeling of slender reinforced concrete shear wall shaking table tests under high-frequency ground motions. Journal of Earthquake Engineering, Vol. **17**, No. 4: pp. 517-542.

NZS 3101:2006 (2006). Concrete Structures Standard. Wellington, New Zealand, Standards New Zealand.

Park, R. (1988). Ductility evaluation from laboratory and analytical testing. Proceedings of the 9th world conference on earthquake engineering.

Park, R., Priestley, M. J. N. and Gill, W. D. (1982). DUCTILITY OF SQUARE-CONFINED CONCRETE COLUMNS. ASCE J Struct Div, Vol. **108**, No. ST4: pp. 929-950.

Sritharan, S., Beyer, K., Henry, R. S., Chai, Y. H., Kowalsky, M. and Bull, D. (2014). Understanding poor seismic performance of concrete walls and design implications. Earthquake Spectra, Vol. **30** No. 1: pp. 307-334.
Structural Engineering Society of New Zealand (SESOC) (2011). Preliminary observations from Christchurch earthquakes. http://canterbury.royalcommission.govt.nz/documents-by-key/20111205.1533, Report prepared for the Canturbury Earthquakes Royal Commission
Wong, S. M. and Vecchio, F. J. (2003). VecTor2 and formworks user's manual. Toronto (Canada), University of Toronto.